AIAA JOURNAL
Vol. 40, No. 9, September 2002

Effects of Pressure-Sensitive Paint on Experimentally Measured Wing Forces and Pressures

Edward T. Schairer,* Rabindra D. Mehta,† and Michael E. Olsen‡
NASA Ames Research Center, Moffett Field, California 94035

Recent experiences with pressure-sensitive paint have shown that very thin paint layers on wind-tunnel models tested at high Reynolds numbers can significantly alter the pressure distributions, and thus the forces and moments, on the models. This was observed during two tests of transport-like wings: a "clean" supercritical wing at transonic cruise conditions in the NASA Ames High Reynolds Number Channel 2 and a high-lift wing, complete with slats and flaps, at landing conditions in the NASA Ames 12-Foot Pressure Wind Tunnel. The effect of paint on the cruise wing was to displace the shock wave slightly upstream from its no-paint position. Smoothing the paint, and even removing it entirely from the leading edge, decreased this displacement slightly. Applying paint to only the slats of the high-lift wing caused the wing to stall prematurely at the highest Reynolds number. This effect could be eliminated by smoothing the paint. Adding paint to other parts of the model had little effect. Paint intrusiveness was much smaller and more ambiguous at lower Reynolds numbers. In both tests, paint intrusiveness occurred because the model surfaces were rougher when they were painted than when they were not, and this additional roughness altered the development of the turbulent boundary layers.

Nomenclature

b	=	model span
C_f	=	skin-friction coefficient
C_l	=	lift coefficient
C_p	=	pressure coefficient
c	=	chord length
c_{mac}	=	mean aerodynamic chord
h	=	paint thickness
k	=	roughness height
k_s	=	equivalent sand grain roughness height
k_s^+	=	$k_s u_\tau/\nu$ equal to $k_s R_u\sqrt{(C_f/2)}$
M	=	Mach number
P_t	=	total pressure
R	=	Reynolds number, $U \cdot c_{\text{mac}}/\nu$
R_u	=	unit Reynolds number, U/ν
R_x	=	$U \cdot x/\nu$
Ra	=	average roughness
t	=	airfoil thickness
U	=	freestream velocity
u	=	streamwise velocity at height k in boundary layer
u_e	=	streamwise velocity at the edge of the boundary layer
u_τ	=	friction velocity, $(\tau_w/\rho)^{1/2}$
x	=	streamwise distance from leading edge
y	=	spanwise distance or distance perpendicular to surface
α	=	angle of attack, deg
ν	=	kinematic viscosity
ρ	=	density
τ_w	=	skin friction

Received 28 July 2001; revision received 28 January 2002; accepted for publication 4 February 2002.

*Aerospace Engineer, Aeronautical Projects and Programs Office, MS 260-1.

†Research Scientist, Aeronautical Projects and Programs Office, MS 260-1. Associate Fellow AIAA.

‡Research Scientist, Numerical Aerospace Simulation Systems Division, MS T27B-1. Associate Fellow AIAA.

Introduction

THE pressure-sensitive paint (PSP) technique for measuring pressure distributions on wind-tunnel models requires coating the surface of the model with special paint that luminesces when it is exposed to light of appropriate frequency. Because the intensity of the luminescence varies inversely with pressure, the pressure distribution can be inferred from the paint intensity distribution, which can be measured by imaging the model.[1,2] The technique has the potential to eliminate the need for pressure taps in wind-tunnel models while yielding pressure measurements over entire surfaces rather than just at discrete points. The success of the method depends, however, on the paint layer being thin and smooth enough that it does not alter the flow over the model, that is, the paint must not be intrusive.

Paint coatings can alter the airflow over a model and thus, become intrusive by 1) changing the actual shape of the model, for example, by adding local thickness, and 2) changing the effective shape of the model, for example, by altering the boundary-layer development and, thus, changing the shape of the inviscid stream surfaces. The first effect can be caused by perfectly smooth coatings; the second is likely to be caused by changing the roughness of the model, for example, by prematurely tripping a laminar boundary layer or by thickening an already turbulent boundary layer. Pressure taps may give a false indication of intrusiveness if the paint alters the surface topology near the taps, for example, by rounding corners of the tap's profile or forming a volcano around the tap.[3]

Surface roughness does not affect the development of a fully turbulent boundary layer, that is, the surface is hydraulically smooth, unless the roughness elements protrude through the viscous sublayer. Schlichting[4] showed that this first occurs when the "equivalent sand-grain roughness" height expressed in boundary-layer units, k_s^+, is about 5. Skin friction begins to show a dependence on roughness diameter in the "transitional" roughness regime $5 < k_s^+ < 70$, and it depends on roughness height alone, independent of Reynolds number, in the "completely rough" regime ($k_s^+ > 70$). Schlichting also defined a simple "admissible roughness" criterion based solely on R_u. Similarly, the roughness likely to "trip" a laminar boundary layer can be estimated from an equivalent roughness Reynolds number.[5–9]

Some early PSP reports included observations about differences between paint-off and paint-on pressure data,[10–13] but none of these offered more than conjecture about the causes of these differences. More recent studies have attempted to explain intrusiveness using measurements of paint roughness and thickness. Vanhoutte et al.[14] found that, in low-speed tests of a swept wing, paint roughness altered or eliminated a separation bubble and, thus, reduced the drag. Also, in transonic tests of a supercritical airfoil, drag increased

with paint roughness, as would be expected if the paint roughness thickened the boundary layer. Mebarki et al.[15] observed that pressure paint on a swept, high-aspect-ratio wing at transonic Mach numbers triggered premature transition to turbulence of the laminar boundary layer. In another test, Mebarki et al.[16] found that, at high Reynolds number and lift, the shock wave on an unswept wing was farther upstream for smoother paints than for rougher paints. Amer et al.[17] measured negligible effect of pressure paint on integrated forces and moments in two tests: a delta-wing model tested at Mach 0.2, and a semispan arrow-wing model tested at Mach 2.4. The paint used in these tests, however, was actually smoother than the unpainted model.

Other studies of wing contamination and surface finish are germane to the problem of pressure-paint intrusiveness. A British experiment[18] before World War II showed a marked decrease in maximum lift and increase in drag of two-dimensional airfoils contaminated by grit at Reynolds numbers where the contamination exceeded Schlichting's admissible roughness criterion. In a wartime British experiment,[19] the drag of an airfoil coated with camouflage paint increased significantly when the paint was rough. Many studies[20–31] have shown that blade surface roughness limits the performance of turbomachinery at high Reynolds numbers. Icing research[32–35] has shown that the maximum lift of wings decreases even at the smallest roughness scales typical of accumulated ice. Icing roughness scales, however, are much greater than what is typical for pressure paints. Another class of wing-contamination research[5–9] deals with tripping laminar boundary layers, that is, prematurely forcing transition to turbulence. As with the icing research, such trips are typically much coarser than the roughness due to pressure paint.

This paper is a substantially revised version of Ref. 36. It reports two recent tests in which the intrusiveness of pressure paint was studied. In both tests, the models were swept, semispan wings typical of commercial transport aircraft, and both tests were conducted in pressurized wind tunnels at high Reynolds numbers. In the first test, paint intrusiveness was measured on a single-element wing at transonic cruise and cruise-buffet conditions. The second test was conducted on a high-lift, multielement model at landing conditions. Although the data reported here are identical to those presented in the original paper, we believe that this paper interprets the paint roughness measurements more correctly, resulting in substantially different conclusions than those of the original paper.

Apparatus

Cruise Wing

The cruise wing[37] was tested in the NASA Ames Research Center High Reynolds Number Channel 2 (Ref. 38). This is a transonic, blowdown wind tunnel capable of operating at total pressures of up to about 6.9 bar. All four walls of the test section (0.61 m high × 0.51 m wide × 3 m long) are solid, straight, and rigid. The top and bottom walls each diverge from the tunnel centerline by 0.2 deg to compensate for the displacement effect of boundary layers on all four walls. The model was supported on a turntable mounted in one sidewall. Mach number is controlled by the height of speed flaps that form a choked throat between the test section and the diffuser.

Air is supplied to the wind tunnel from the NASA Ames Research Center 207-bar (3000-psi) air system. Typical runs at Mach 0.8 and $P_t = 6.9$ bar lasted 60–90 s before the supply pressure became too low to maintain the P_t setpoint. The total temperature of the flow was typically about 255 K (460°R) and decreased slowly throughout each run. The unit Reynolds number at these conditions was $R_u = 108 \times 10^6$/m (33×10^6/ft).

The model (Fig. 1) was a semispan wing designed to produce pressure distributions typical of advanced supercritical transport wings at transonic cruise. Thickness-to-chord ratio t/c was about 0.15, the wing was constructed of stainless steel, and its surfaces were highly polished. The model was instrumented with 28 pressure taps arranged in five chordwise rows on the upper surface. Taps circled and numbered in Fig. 1 will be referred to subsequently.

The tap pressures were measured by electronically scanned differential pressure transducers [PSI, ±3.10 bar (±45 psid)]. The range of samples for which flow conditions were steady was identified after each run by analyzing time histories of total and static pressure measurements. Statistical quantities for each tap (mean, variance, and 95% range) were computed from samples within this range. At maximum mass-flow rates, reduced pressures were based on 100–140 samples from each tap.

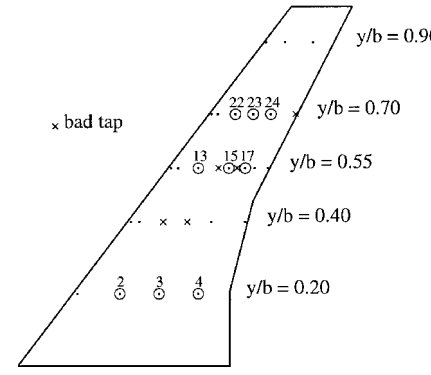

Fig. 1 Planform of cruise wing showing locations of pressure taps: span = 0.3048 m, c_{mac} = 0.127 m, and LE sweep = 36.9 deg.

Fig. 2 Schematic of high-lift wing: b = 1.18 m, c_{mac} = 0.353 m, and sweep ~ 35 deg.

PSP data were acquired by imaging the painted model through a window in the top wall of the test section with a 14-bit scientific-grade digital camera. The model was illuminated by ultraviolet lamps through the same window.

Flow over the cruise wing was also simulated numerically using a Reynolds averaged Navier–Stokes (RANS) code with the Spalart–Allmaras turbulence model (see Ref. 37).

High-Lift Wing

The high-lift wing was tested in the NASA Ames Research Center 12-Foot Pressure Wind Tunnel (URL: http://windtunnels.arc.nasa.gov). This is a closed-return wind tunnel capable of operating at subsonic Mach numbers and total pressures of up to 6.1 bar. The circular test section is 3.65 m (12 ft) in diameter, and all walls are solid. For the present semispan model test, a horizontal splitter plate was installed above the floor of the test section and served as an image plane. Flaps at the downstream end of the splitter plate were set to minimize the streamwise Mach gradient in the channel above the plate.

The model was a low-wing-transport, wing–body configuration. Full details cannot be presented because the design is proprietary. The wing was swept, tapered, and twisted and was equipped with leading-edge slats, two-element trailing-edge flaps, ailerons, and an engine pylon and flow-through nacelle. For the present tests, the slats and flaps were set for a landing configuration (shown schematically in Fig. 2). The model was constructed from a variety of materials including brass, magnesium, steel, and aluminum. It was a veteran of many tests, and none of its surfaces was particularly smooth.

The model was supported by a force-and-moment balance with 26.7 kN (6000 lbf) normal-force capacity. The wing, slats, and flaps were instrumented with over 200 pressure taps arranged in chordwise rows at four span stations. These were connected to ±1.03 bar (±15 psid) PSI differential pressure transducers located in the body of the model. Signals from strain gauges in the balance and pressure transducers were input to a 16-bit analog-to-digital converter and were sampled at a rate of approximately 3000 samples/s. Each measurement was averaged over 3000–6000 samples. No PSP data were acquired during the paint-intrusiveness phase of this test.

Paint

The models were painted with pressure paint developed at the University of Washington.[39] Two coats of paint are normally applied: a white base coat and a top coat that carries the active light- and pressure-sensitive molecule. The binder for both coats is a

proprietary polymer called FIB. Both coats are mixed with solvents that allow them to be applied with a spray gun and also promote a smooth finish. While the paints were being sprayed, air was very gently blown through the model pressure taps to prevent the paint from clogging the taps. The paints dried to a hard surface within a few minutes.

Paint thickness was measured using a PosiTector 6000-FN2 coating-thickness gauge that uses the magnetic principle to measure the thicknesses of nonmagnetic coatings on ferrous materials, for example, the cruise wing. This gauge can also measure thickness of paint on nonferrous surfaces (various elements of the high-lift wing) using the eddy current principle. The average paint roughness was measured with a Surtronic 10 surface-roughness gauge. This gauge drags a stylus across a surface and determines the average absolute value of the normal deviation from the mean deviation over the evaluation length, *Ra*. The radius of the stylus was 5 μm. The specified resolution is 0.1 μm (4 μin.). In some cases the paints were smoothed using a 3M 9-μm-grade Micro Finishing film.

Results

Paint intrusiveness was measured by comparing data from runs with and without paint at the same conditions. For the cruise wing, only pressure-tap measurements could be compared; for the high-lift wing, balance data were available as well. Because the data for the high-lift wing are proprietary, they are shown without scales on the graphs. Test conditions for the two wings are summarized in Table 1.

Cruise Wing

The upper surface of the cruise wing was painted with both base and top coats. Several runs were made before anything was done to reduce the intrusiveness of the paint (rough paint). Then, the paint along the leading edge of the model was lightly polished. Next, the paint was entirely polished away from the leading edge (LE) (stripped LE) to a line just aft of the most-upstream pressure taps, $x/c = 0.03$. Finally, the entire upper surface of the model was vigorously polished until there was no further improvement in measured smoothness (smooth or maximum buff paint). This left just enough top coat to allow acquisition of PSP data. Paint thickness and surface roughness data for the cruise wing are summarized in Table 2.

At the design cruise condition ($M = 0.80$, $\alpha = 1.75$ deg, and $R = 13.6 \times 10^6$), there was a strong shock wave on the upper surface of the model at about midchord. As angle of attack increased, the shock wave moved upstream, and the magnitude of the suction peak upstream of the shock increased. At $\alpha = 2.25$ deg, the boundary layer on the upper surface was just beginning to separate, and at the two highest angles it was fully separated downstream of the shock wave. These trends are evident in the pressure-paint images (Fig. 3).

We expected the flow to be most sensitive to the presence of paint along the LE of the model because of the thin boundary layer in that region. In Fig. 3, the paint had been polished away from the LE: Note that the most-upstream pressure taps (the taps are shown as white dots) are just upstream of the paint line. When the LE was painted, it soon became pitted, and these pits, being in a supersonic region of flow, generated Mach waves. These are evident as cross hatching in Fig. 4, a PSP image at the design cruise condition where the gray scale has been expanded (C_p range ~ 0.2) to make the Mach waves more visible.

Most runs (19) were at the design cruise condition. Fewer runs were made when either Reynolds number R or α was offdesign (5-6 per condition). Only two runs (one paint-off and one paint-on run)

Table 1 Test conditions for cruise and high-lift models

Parameter	Cruise wing	High-lift wing
M	0.80[a]	0.23
$R \times 10^6$	7.3, 11.3, 13.6[a]	3.4, 5.2, 6.7
α, deg	1.75,[a] 2.25, 2.75, 3.75	0-stall

[a]For design point.

Table 2 Summary of paint configurations on cruise wing

Configuration	*Ra*, μm	*h*, μm	x/c
No paint	0.05–0.1	0	
Paint rough (unbuffed)	1.0–1.5	10–20	>0
Paint rough (stripped LE)	1.0–1.5	10–20	>0.03
Paint smoothed (maximum buff)	0.5–0.76	10–15	>0.03

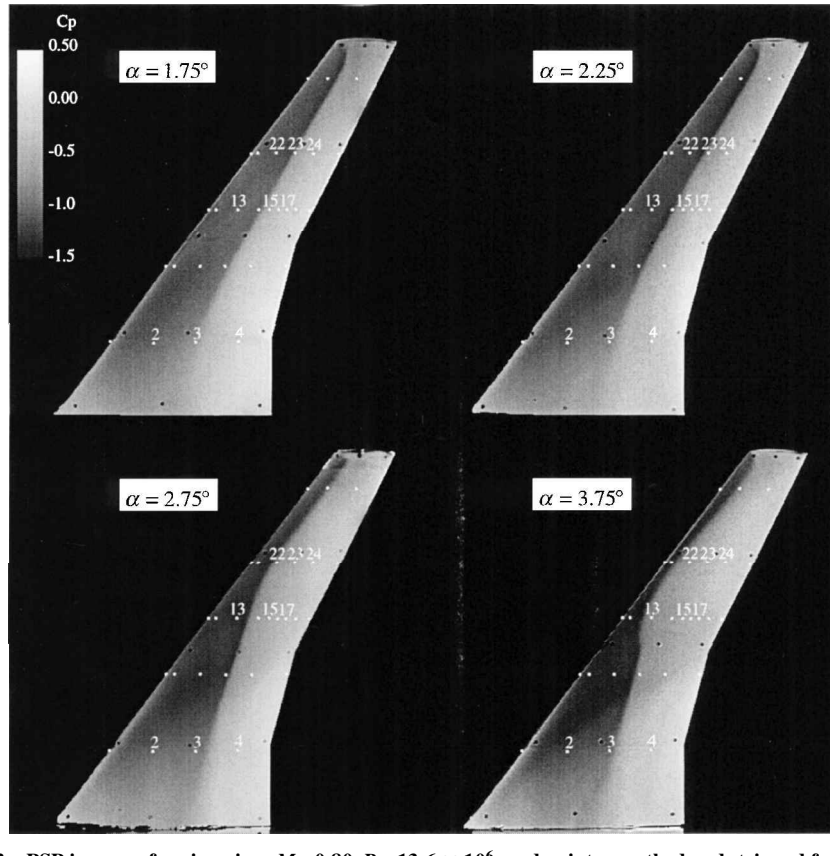

Fig. 3 PSP images of cruise wing: $M = 0.80$, $R = 13.6 \times 10^6$, and paint smoothed and stripped from LE.

were made at each condition where both Reynolds number R and α were offdesign.

Design Cruise Condition

There was considerable scatter in the pressure-tap data from one run to the next, which made it difficult to identify small changes due to the presence of paint. For example, Fig. 5 shows pressure coefficients for two paint-off and two paint-on runs at nominally the same design cruise condition. Error bars indicate the range of 95% of the samples from each run. Differences between the paint-off and paint-on data are not much larger than differences between data from the two paint-off runs. The scatter and error bars were especially large at pressure taps near the shock wave. Several factors contributed to this scatter. The model never fully reached static equilibrium even after steady freestream conditions had been established, probably because of thermal warping. This warping was apparent from measurements of the deflection of the wingtip,[36] which increased very slowly throughout each run, and from time histories of pressures from pressure taps near the shock wave (taps 3, 15, and 23 in Figs. 1 and 3), which increased monotonically throughout each run, indicating that the shock wave was creeping upstream. This shock movement was also independently observed in sequences of pressure-paint images acquired during paint-on runs. The effects of thermal warping were smaller when the model was already cold. Therefore, our standard run procedure was to precool the model by preceding each data run with two short cooling runs. The data shown in Fig. 5 were acquired after precooling the model.

Another factor affecting the repeatability of the data was small differences in Mach number from one run to the next. The standard deviation of average freestream Mach numbers from 19 runs at the design cruise condition was 0.001. This is more than 10 times as large as the statistical variation predicted from the standard deviation of Mach number during each run (typically 0.0007) and the number of samples per run (at least 100). Run-to-run differences in Mach number were unpredictable and occurred even when the settings of the speed flaps had not been changed between runs. Note the differences in Mach number among the runs shown in Fig. 5.

To separate the effects of paint intrusiveness from those due to variations in Mach number, we plotted the pressure data from each tap vs freestream Mach number for all paint-off and paint-on runs. Figure 6 shows typical plots for nine taps: three at each of three span stations, $y/b = 0.20$, 0.55, and 0.70. (Taps are circled and numbered in Fig. 1, and numbered in Fig. 3. Note that the C_p range of the middle row of plots is double that of the top and bottom rows.) Error bars, indicating the range of 95% of the samples, are shown for both Mach number and pressure coefficient. Upstream (Fig. 6a) and downstream (Fig. 6c) of the shock wave, the paint-off data show no correlation with Mach number, and the data repeat within a C_p range of about ± 0.01. Furthermore, at the downstream taps there is no apparent difference between the paint-off and paint-on data. At the two upstream, inboard taps, however, the paint-on pressures are consistently lower than the paint-off pressures. Smoothing the paint appears to have had little effect on the data.

Differences between the paint-off and paint-on data are much larger near the shock wave: The paint-on pressures are systematically higher, indicating a slightly more upstream position of the shock wave. There is no clear separation between the smooth and rough paint data, except perhaps at $y/b = 0.70$. Finally, at all three span stations, both the paint-off and paint-on data show a correlation with Mach number: The pressure is lower at higher Mach numbers, indicating a more downstream shock-wave position.

Average paint-off and paint-on pressures were computed by fitting the C_p vs Mach data at each tap by a straight line (shown as broken lines in Fig. 6) and then determining from each line the pressure at the (arbitrary) reference Mach number. At taps where there was no correlation with Mach number, that is, nearly all taps except those near the shock wave, this was equivalent to simply averaging the data. Resulting paint-off and paint-on average pressure distributions are compared in Fig. 7. The error bars show the standard deviation of the data about the curve fit at each tap. Smooth and rough paint-on data are shown separately. The biggest effect of the paint was to move the shock wave slightly upstream. Adding paint also appears to have slightly increased the suction upstream of the shock wave. Recovery pressures downstream of the shock wave were unaffected by the paint.

The rms scatter in C_p of the paint-off data from all 23 taps relative to the paint-off C_p vs Mach trend lines was 0.013. This decreased to 0.006 when data from the three taps nearest the shock wave were excluded. Local differences between the paint-off and paint-on pressures at each tap were quantified by computing the mean difference between each paint-on data point and the linear best fit of the paint-off data (broken lines in Fig. 6). A global measure of the difference was then determined by computing the rms of the

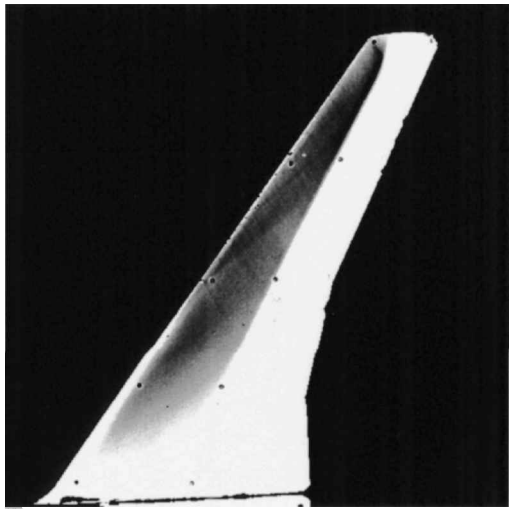

Fig. 4 PSP image of cruise wing showing Mach waves generated by pits in paint along the LE.

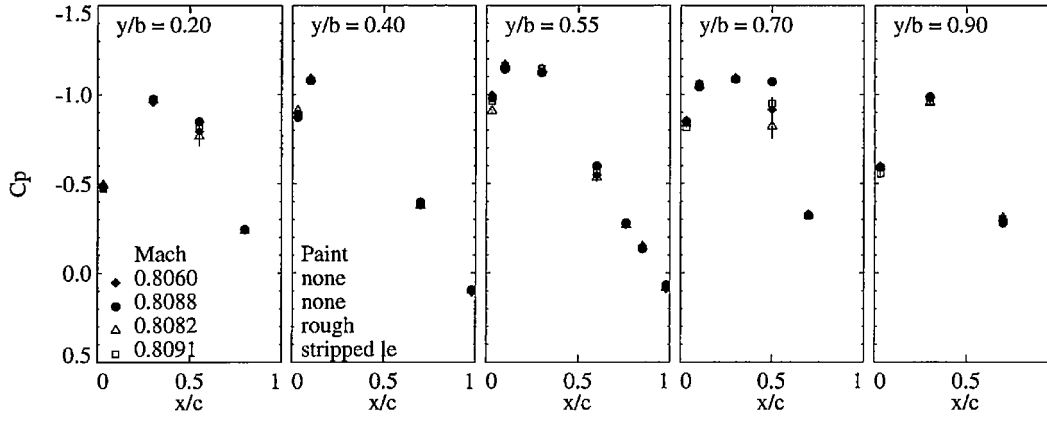

Fig. 5 Paint-off vs paint-on pressures on cruise wing at design cruise conditions.

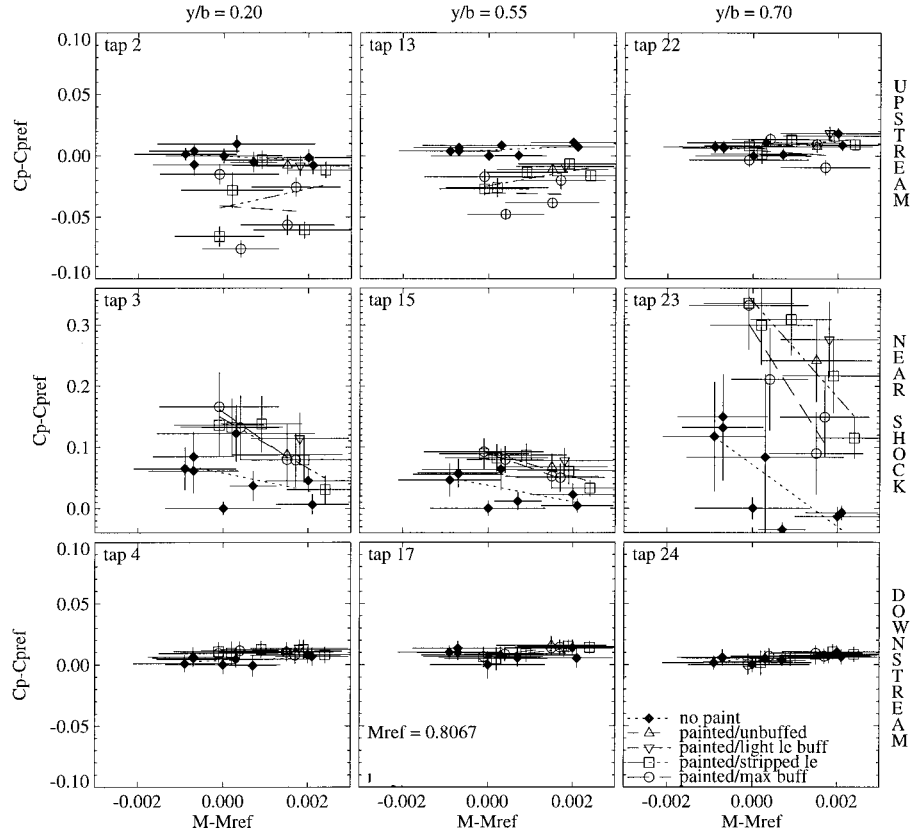

Fig. 6 Pressure coefficients vs Mach number for selected taps; cruise wing at design cruise conditions.

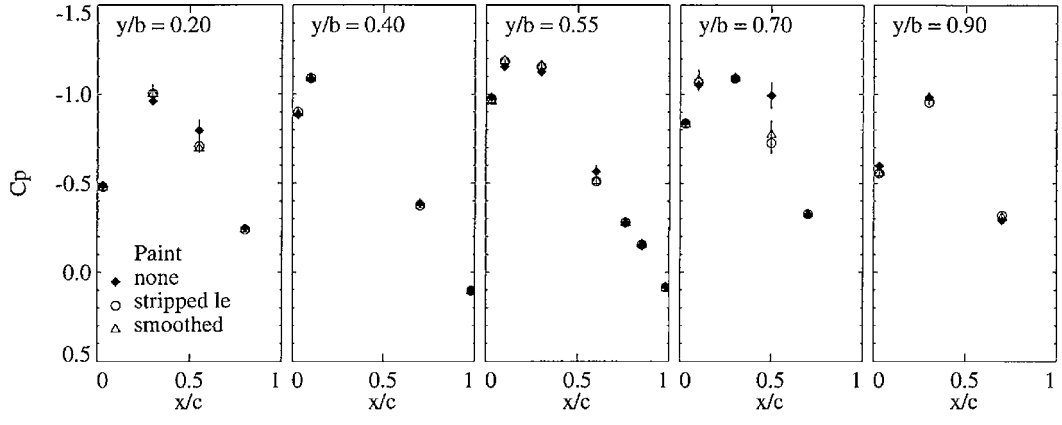

Fig. 7 Paint-off vs paint-on pressures corrected for Mach variations: $M = 0.8067$ and cruise wing at design cruise conditions.

average differences at all taps. This method yields zero for data randomly scattered about the paint-off trends and a positive number for data that differ systematically from the paint-off trends. By this metric, the difference in C_p between the paint-off and paint-on data at the design cruise condition was about 0.05 including data from all useable taps; excluding data from the three taps near the shock wave, where differences were much larger, yielded a difference in C_p of about 0.015.

Off-Design Conditions

The trends at lower (off-design) Reynolds numbers were very much the same as those at the design condition: The largest differences between the paint-off and paint-on data occurred at taps near the shock wave where the paint-on pressures were slightly higher, indicating a more-forward shock position; there was a slight increase in the suction upstream of the shock wave. When data from the three pressure taps near the shock wave were excluded, the paint-intrusiveness metric already described was approximately the same at the lower Reynolds numbers as it was at the design Reynolds number ($\Delta C_p \approx 0.015$).

The magnitude of paint intrusiveness was about the same at off-design angles of attack. However, trends were less clear for these more complex, nearly and fully separated flows. In addition, detecting trends was more difficult because fewer runs were made at these conditions.

High-Lift Wing

The test strategy for the high-lift wing was to add paint to various elements of the model in incremental steps, and, after each step, test the model over the full range of test conditions (Table 1). Table 3 summarizes this sequence, including paint thickness and roughness. Two sets of runs were made after paint (base coat only) was added to the slats (cases b and c) and wing-box LEs (cases d and e for lower surface and cases f and g for upper surface): the first with the paint in its rough, untreated form and the second after the most

Table 3 Summary of paint configurations on high-lift wing

Case	Legend	Configuration	Comment	*Ra*, μm	*h*, μm
a	None	No paint		0.5	0
b	Slats (R)	Base coat on slats upper	Rough	1.0–1.5	13
c	Slats (S)	surface	Smoothed	0.5–1.0	13
d	+lower wle (R)	Base coat added to wing-box	Rough	1.0–1.5	13
e	+lower wle (S)	lower surface LE ($x/c < 0.03$)	Smoothed	0.5–1.0	13
f	+upper wle (R)	Base coat added to wing-box	Rough	1.0–1.5	13
g	+upper wle (S)	upper surface LE ($x/c < 0.05$)	Smoothed	0.5–1.0	13
h	+flaps (R)	Base coat added to upper and lower surfaces of flaps	Rough	1.0–1.5	13
i	−slats	Base coat removed from slats			
l	None	All paint removed		0.5	0
j	All (slats/le R)	Fully painted wing (base + top	Rough	1.0–1.5	25
k	All (slats/le S)	coats)	Smoothed on slats and wing box LE	0.5–0.75	25

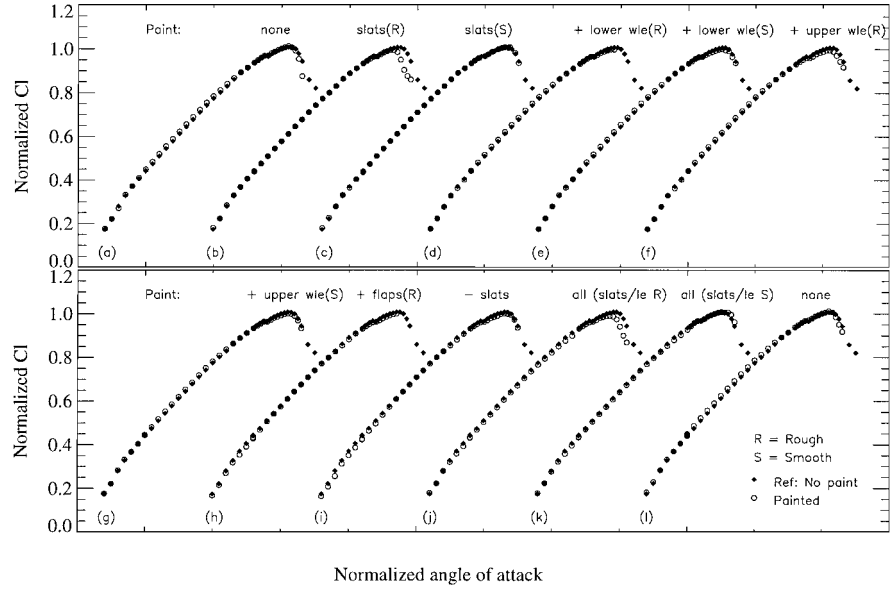

Fig. 8 Paint-off vs paint-on lift curves for high-lift wing: $M = 0.23$ and $R = 6.7 \times 10^6$.

recently applied paint had been smoothed. For the final two steps (cases j and k), all exposed aerodynamic surfaces were painted with both base coat and top coat. The paint was rough for case j, and the paint on the slats and wing-box LE had been smoothed for case k.

Balance Data

Figure 8 shows lift coefficient (normalized by paint-off maximum lift) vs angle of attack (normalized by paint-off stall angle) data from the balance for the full sequence of paint configurations at the highest Reynolds number. Each plot compares data for a different paint configuration (Table 3) to paint-off data. The first (curve a) and last (curve l) curves compare the reference paint-off run to other paint-off runs made at the beginning and end of the sequence. Rough paint on the slats alone resulted in a small but significant decrease in the stall angle (curve b). After this paint was smoothed, however, the lift curve was almost indistinguishable from the paint-off curve (c). Subsequent addition of paint to the wing-box LEs (upper and lower surfaces, rough and smooth) and to the flaps (rough) had very little effect on the lift curves d–h. Likewise, removing the smoothed paint from the slats had little effect (curve i). Finally, after the model was stripped and fully repainted, but before the paint on the slats and wing-box LEs was smoothed, the stall angle again decreased (curve j) in much the same way as it did when only the slats were painted (curve b). Smoothing the paint on the slats and wing-box LEs restored the lift curve to its paint-off form (curve k). The effects of painting the model were inconclusive at lower Reynolds numbers because stall occurred more abruptly and was less repeatable than at the highest Reynolds number.

There were no significant differences in drag or pitching moment measurements between paint-off and paint-on runs below the stall angle.

Pressure Data

Figure 9 is a comparison of paint-off and paint-on pressure-tap data at a condition near the stall angle, where there were significant differences in the balance data. Pressure coefficients C_p are shown vs chordwise position for the upper and lower surfaces of the slats, wing box, and flaps/ailerons at four span stations. (The relative chords of the wing elements are not shown to scale.) The condition shown ($R = 6.7 \times 10^6$, $\alpha/\alpha_{\text{stall}} = 1.09$) corresponds to lift curve b in Fig. 8, where only the slats were painted and the paint was rough. Compared to the paint-off data, the paint-on data show significantly lower suction on the upper surfaces of the slat and wing box at $y/b = 0.37$, which is just outboard of the pylon and nacelle. There were much smaller reductions in suction at span stations farther outboard and inboard. The paint-on pressures are similar to paint-off pressures at a slightly higher angle of attack. Thus, the paint caused premature stalling but did not alter the nature of the stall. After the paint on the slats was polished, the paint-off and paint-on pressures were virtually indistinguishable.

Differences between paint-off and paint-on pressure-tap data at lower Reynolds numbers were about as large as differences between repeated paint-off runs.

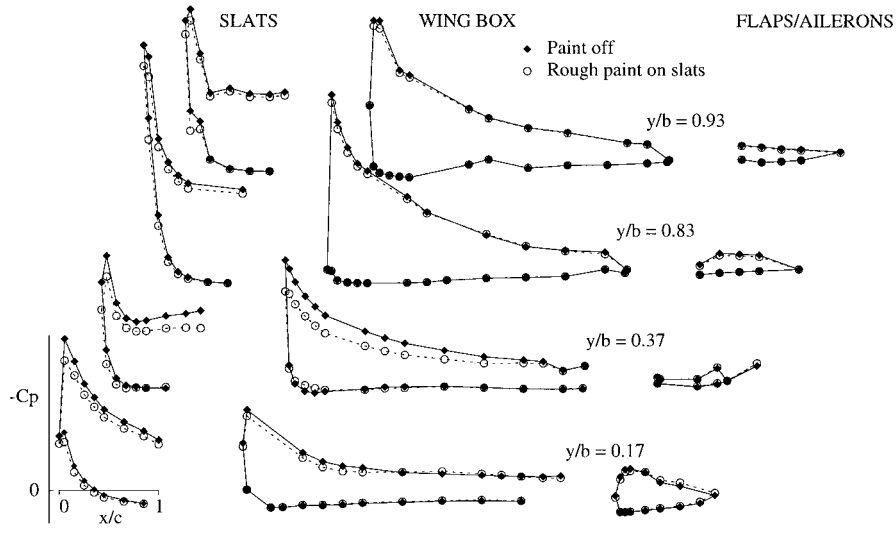

Fig. 9 Paint-off vs paint-on pressure coefficients near stall angle for high-lift wing: $M = 0.23$ and $R = 6.7 \times 10^6$.

Discussion

Differences between paint-on and paint-off data in both tests are clear indications of paint intrusiveness. If these had been false indications (due, for example, to local topological changes at pressure taps) there would have been systematic differences between paint-off and paint-on data at all conditions. This was not the case in either test. Therefore, we must consider thickness and roughness effects.

Thickness Effects

For the cruise wing, the paint increased the thickness-to-chord ratio t/c of the mean aerodynamic chord by less than 0.1%. Numerical simulation indicated that this thickness increase had a negligible effect on the pressure distributions at cruise and cruise-buffet conditions. For the high-lift wing, the increase in t/c of the wing box was much smaller; however, increases in t/c of the high-lift devices were about the same as for the cruise wing, and paint on the LEs of the wing box and flap elements reduced gaps between elements by up to 1%. No computational fluid dynamics simulation of the high-lift wing was available to assess the effects of these thickness changes. However, because paint intrusiveness could be eliminated by polishing the paint without appreciably affecting its thickness, it is unlikely that the additional thickness of paint was responsible for the change in the wing's performance.

Roughness Effects

The measured, average geometric roughness of a surface, Ra, is, in general, quite different than the equivalent sand-grain roughness k_s defined by Schlichting. Several investigators have tried to establish general relationships between Ra, k, and k_s. Young[19] estimated $k_s/k = 1.6$ for camouflage paint, and Koch and Smith[23] pointed out that, for a surface with a profile that lies between a sinusoid and saw-toothed, this corresponds to $5.0 < k_s/Ra < 6.4$. Based on their own fluid dynamic and profilometer measurements of standard sand papers, Koch and Smith estimated that $k_s/k = 1.5$ and $k_s/Ra = 6.2$, in good agreement with Young's result. Measurements by other researchers, however, have shown greater variations: Schaffler[24] estimated $k_s/Ra = 8.9$, and Acharya et al.[30] measured $4.2 < k_s/Ra < 10$ for various types of roughness. Vanhoutte et al.[14] found that k_s is greater than Ra but less than the maximum roughness height, which in their experiments was 10–50 times Ra. Lacking better information, we adopt Koch and Smith's result, $k_s/Ra = 6.2$, in this paper.

We first consider if the paint forced premature transition to turbulence of a laminar boundary layer. The roughness required to trip a laminar boundary can be estimated[5–9] from a roughness Reynolds number, $R_k = k \cdot u/\nu = k \cdot R_u \cdot (u/u_e) \cdot (u_e/U) = 600$. An upper bound on R_k for a given k and R_u can be determined by assuming maximum values for the remaining two terms, u/u_e and u_e/U. The maximum value of u/u_e is 1.0, and the maximum value of u_e/U can be estimated from freestream conditions and

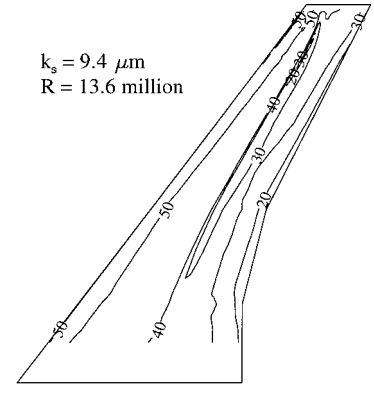

Fig. 10 Contour plot of k_s^+ for cruise wing at design cruise conditions: $k_s = 9.4$ μm and $R = 13.6 \times 10^6$.

C_p at the point of minimum pressure (where u_e is greatest). If, following Koch and Smith,[23] we assume $k/Ra = (k_s/Ra)/(k_s/k) = 6.2/1.5 = 4.133$, then, for rough paint at the maximum Reynolds numbers $(R_k)_{\max} \approx 1166 > 600$ for the cruise wing and $(R_k)_{\max} \approx 377 < 600$ for the high-lift wing.

These estimates indicate that the unpolished paint was rough enough to force transition on the cruise wing but not on the high-lift wing. It is unlikely, however, that there was significant laminar flow in either case at the conditions where intrusiveness was observed. Oil-film skin-friction measurements on the unpainted cruise wing indicated that the boundary layer was fully turbulent virtually all the way to the LE.[37] This conclusion is supported by the very small effects that polishing the paint, and even stripping it from the LE, had on the pressure distributions. For the high-lift wing at angles near stall (the only condition where intrusiveness was evident), the very steep adverse pressure gradient near the LE of the slats (Fig. 9) most likely would have resulted in boundary-layer transition regardless of the presence of paint.

We next consider the effects of surface roughness on a fully developed, turbulent boundary layer. The equivalent sand-grain roughness height in boundary-layer units is given by $k_s^+ = k_s R_u \sqrt{(C_f/2)}$. For the cruise wing, we used the C_f distribution computed by the RANS code, which was for a smooth surface and was in good agreement with oil-flow interferometry measurements.[37] When $k_s = 6.2 \cdot Ra$ was assumed, the entire upper surface of the unpainted wing was hydraulically smooth ($k_s^+ < 5$) even at the highest unit Reynolds number R_u. The k_s^+ distribution for the painted wing at the design cruise condition is shown in Fig. 10. This result is based on k_s for rough paint and C_f for a smooth surface (RANS solution). Therefore, it is a low estimate because it ignores the higher

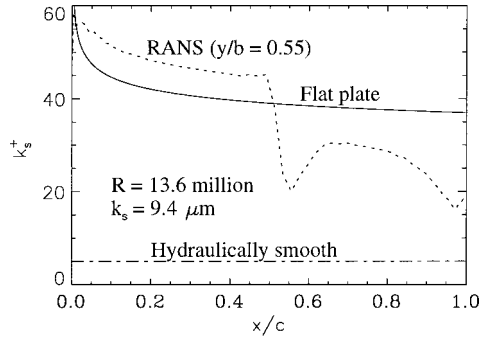

Fig. 11 Distribution of k_s^+ along $y/b = 0.55$ of cruise wing at design cruise conditions, rough paint.

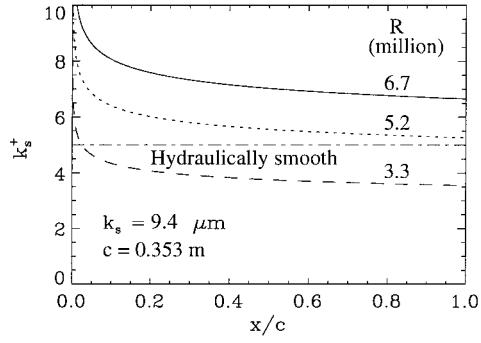

Fig. 12 Distribution of k_s^+ along a flat plate at test conditions of high-lift wing.

C_f on surfaces that are not hydraulically smooth. At design cruise conditions, the entire wing is in the intermediate regime between hydraulically smooth and completely rough ($5 < k_s^+ < 70$). Smoothing the paint reduced Ra (and, thus, k_s and k_s^+) by about half, but the surface was still in the intermediate regime. To first order, k_s^+ is also proportional to unit Reynolds number R_u. Therefore, for smooth paint at the lowest unit Reynolds number ($R_u = 57.4 \times 10^6$/m), the k_s^+ distribution in Fig. 10 would be reduced by a factor of about four (two each for reductions in roughness and Reynolds number). At this condition the paint was still not hydraulically smooth.

Figure 11 shows the chordwise distribution of k_s^+ at about midspan of the cruise wing ($y/b = 0.55$) for the same conditions as Fig. 10 ($Ra = 1.5$ μm and $R = 13.6 \times 10^6$). A large decrease in k_s^+ occurs at the shock wave, corresponding to a reduction in skin friction. Figure 11 includes an estimate of k_s^+ for fully turbulent flow over a smooth flat plate at the same conditions computed using Schlichting's empirical equation[4] $C_f = (2 \log R_x - 0.65)^{-2.3}$. This much simpler estimate is in good agreement with the general levels of k_s^+ computed from the RANS solution.

Because a RANS solution of flow over the much more complex high-lift wing was not available, the k_s^+ distribution for rough paint along the mean aerodynamic chord was estimated using k_s of the paint and C_f for a smooth flat plate determined as described earlier. These estimates indicate that, at the highest Reynolds number ($R = 6.7 \times 10^6$), the unpolished paint was slightly rougher than a hydraulically smooth surface (Fig. 12). Smoothing the paint reduced k_s^+ by half and brought nearly the entire surface below the hydraulically smooth threshold. At the lowest Reynolds number ($R = 3.4 \times 10^6$), even the rough paint was hydraulically smooth, except perhaps very near the LE. The bare wing, which was about three times as smooth as the rough paint, was hydraulically smooth at all Reynolds numbers.

Schlichting's admissible roughness criterion,[4] $k_{s_{adm}} = 100/R_u$, is an even simpler way to assess surface roughness. (Without explanation, Schlichting drops the distinction between k and k_s in his discussion of admissible roughness. Consistency with the concept of hydraulic smoothness, however, requires that admissible roughness refers to equivalent sand-grain roughness k_s.) This criterion is independent of the streamwise length of an object and amounts to a

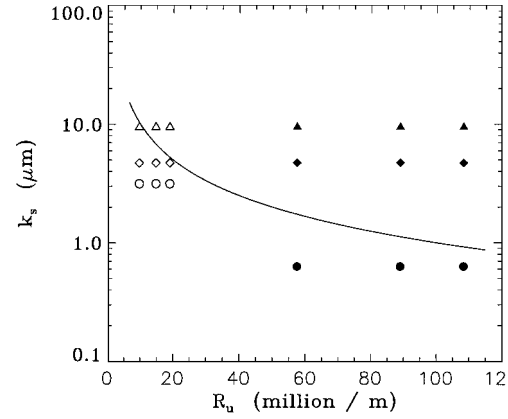

Fig. 13 Admissible roughness vs unit Reynolds number: solid line, $k_s = 100/R_u$; open symbols, high-lift wing; closed symbols, cruise wing; triangles, rough paint; diamonds, smooth paint; and circles, no paint.

critical roughness Reynolds number of 100. (Koch and Smith[23] and Schaffler[24] found that, for turbomachinery, the critical roughness Reynolds number, where losses begin to depend on k_s, is about 90. When the uncertainty in the relationship between k_s and Ra is considered, this is quite close to Schlichting's value of 100.) Figure 13 is a comparison of roughnesses of the high-lift (open symbols) and cruise (filled symbols) wings to the admissible roughness (solid line). For the cruise wing, both the unpolished (triangles) and polished (diamonds) paint exceeded the admissible roughness at all Reynolds numbers, whereas the roughness of the unpainted wing (circles) was always less than the admissible roughness. Unpolished paint on the high-lift wing exceeded the admissible roughness at the two highest Reynolds numbers and was just below the threshold at the lowest Reynolds number. Polishing the paint brought k_s below the admissible roughness at all Reynolds numbers. Even though the unpainted surface of the high-lift wing was much rougher than that of the cruise wing, it was still smoother than the admissible roughness at all conditions.

The hydraulic smoothness and admissible roughness analyses are consistent with each other and with the paint intrusiveness observed in both tests. Both wings were hydraulically smooth without paint, but were in the intermediate roughness regime when they were covered with unpolished paint (except at the lowest Reynolds number of the high-lift test, where the paint was hydraulically smooth). Polishing the paint did little to reduce the intrusiveness on the cruise wing because the polished paint was still not hydraulically smooth, even at the lowest Reynolds number. This conclusion holds even if the k_s levels are increased or decreased by 50%. At the lower unit Reynolds numbers of the high-wing test, boundary layers were thicker, and the paint was much closer to being hydraulically smooth. At the highest Reynolds number of that test, polishing the paint brought the surfaces from just above to just below the hydraulically smooth threshold. The resulting change in boundary-layer development was important only on the slats near the critical condition of stall. The effect was small at the lowest Reynolds number because the unpolished paint was already hydraulically smooth. Conclusions about the high-lift wing are more sensitive to the uncertainty in the roughness measurements than for the cruise wing because the measured roughness was more nearly equal to the admissible roughness (Fig. 13).

In both tests, paint intrusiveness was not large and was only evident by measuring quantities that are very sensitive to boundary-layer development: shock-wave position for the supercritical cruise model and stall angle for the high-lift model. Nonetheless, intrusiveness was large enough to obscure the true effects of Reynolds number on important aerodynamic characteristics of the models. This is a serious problem that must be considered in all PSP applications, particularly those at high unit Reynolds numbers.

Conclusions

The presence of pressure paint on the cruise wing caused the position of the shock wave (an extremely sensitive indicator of small changes between runs for a supercritical wing) to shift slightly

upstream from its paint-off position over the range of Reynolds numbers tested. This effect persisted even after the paint was first smoothed and then removed entirely from the LE. This probably occurred because the painted surface was not hydraulically smooth, whereas the unpainted model was. The stall angle of the high-lift wing at the highest Reynolds number decreased slightly when rough paint was applied only to the LE slats and returned to its paint-off value after this paint had been smoothed. This probably occurred because smoothing the paint brought the surface roughness from above to below the hydraulically smooth threshold. Paint intrusiveness was lower at the lowest Reynolds number because even the unsmoothed paint was hydraulically smooth. These results show that, when pressure paint is used at high unit Reynolds numbers, the true effect of Reynolds number may be obscured by paint intrusiveness if the roughness of the painted surface is different from that of the model, except if both the painted and unpainted surfaces are hydraulically smooth.

Acknowledgments

The authors are grateful to James D. McLean of The Boeing Commercial Airplane Company for his constructive comments about our original paper. These comments led to reinterpretation of the roughness data and substantially different conclusions. We also thank Patricia Whittaker of NASA Ames Research Center for her help in retrieving the balance and pressure data from the high-lift test. Finally, we thank James Bell, Lawrence Hand, and Daniel Morgan of NASA Ames Research Center for their assistance during both tests.

References

[1]McLachlan, B. G., and Bell, J. H., "Pressure-Sensitive Paint in Aerodynamic Testing," *Experimental Thermal and Fluid Science*, Vol. 10, No. 4, 1995, pp. 470–85.

[2]Bell, J. H., Schairer, E. T., Hand, L. A., and Mehta, R. D., "Surface Pressure Measurements using Luminescent Coatings," *Annual Review of Fluid Mechanics*, Vol. 33, 2001, pp. 155–206.

[3]Benedict, R. P., *Fundamentals of Temperature, Pressure, and Flow Measurements*, Wiley, New York, 1984, pp. 339–370.

[4]Schlichting, H., *Boundary-Layer Theory*, 6th ed., McGraw–Hill, New York, 1968, pp. 596–623.

[5]von Doenhoff, A. E., and Horton, E. A., "A Low-Speed Experimental Investigation of the Effect of a Sandpaper Type Roughness on Boundary-Layer Transition," NACA TN 3856, Oct. 1956.

[6]Smith, A. M. O., and Clutter, D. W., "The Smallest Height of Roughness Capable of Affecting Boundary Layer Transition," *Journal of the Aerospace Sciences*, Vol. 26, No. 4, 1959, pp. 229–245.

[7]Braslow, A. L., and Knox, E. C., "Simplified Method for Determination of Critical Height of Distributed Roughness Particles for Boundary-Layer Transition at Mach Numbers from 0 to 5," NACA TN 4363, Sept. 1958.

[8]Braslow, A. L., "Review of the Effect of Distributed Surface Roughness on Boundary-Layer Transition," Rept. 254, AGARD, April 1960.

[9]Braslow, A. L., Hicks, R. M., and Harris, R. V., "Use of Grit-Type Boundary-Layer-Transition Trips on Wind-Tunnel Models," NASA TN D-3579, Sept. 1966.

[10]Engler, R. H., Hartmann, K., and Schulze, B., "Aerodynamic Assessment of an Optical Pressure Measurement System (OPMS) by Comparison with Conventional Pressure Measurements in a High Speed Wind Tunnel," *14th International Congress on Instrumentation in Aerospace Simulation Facilities (ICIASF)*, Rockville, MD, 1991.

[11]Davies, A. G., Bedwell, D., Dunleavy, M., and Brownjohn, N., "Pressure Sensitive Paint Limitations and Solutions," *17th International Congress on Instrumentation in Aerospace Simulation Facilities (ICIASF)*, Pacific Grove, CA, 1997.

[12]Lyonnet, M., Deleglise, B., Grenat, G., Bykov, A., Mosharov, V., Orlov, A., and Fonov, S., "The Two-Component PSP Investigation on a Civil Aircraft Model in S2MA Wind Tunnel," *Advanced Aerodynamic Measurement Technology*, CP-601, AGARD, 1998, pp. 30-1–30-8.

[13]Sellers, M. E., "Pressure Sensitive Paint Data on the Transonic Technology Wing Demonstrator (TST) in the AEDC Propulsion Wind Tunnel 16T," Arnold Engineering Development Center, AEDC TR-98-3, Tullahoma, TN, 1998.

[14]Vanhoutte, F. G., Ashill, P. R., and Garry, K. P., "Intrusion Effects of Pressure Sensitive Paint in Wind-Tunnel Tests on Wings," AIAA Paper 2000-2525, June 2000.

[15]Mebarki, Y., Grenier, M., Ellis, F., and Mokry, M., "PSP Effect on the Flow-Investigation for Ruthenium-based PSP," 7th Annual Pressure-Sensitive Paint Workshop, Purdue Univ., West Lafayette, IN, Oct. 1999.

[16]Mebarki, Y., Grenier, M., and Thain, J., "Comparison of Pressure Sensitive Paints on a Supercritical Wing at Cruise Speed," 9th International Symposium on Flow Visiualization, Heriot-Watt Univ., Edinburgh, Paper 207, 2000.

[17]Amer, T. R., Liu, T., and Oglesby, D. M., "Characterization of Pressure Sensitive Paint Intrusiveness Effects on Aerodynamic Data," AIAA Paper 2001-0556, Jan. 2001.

[18]Jones, R., and Williams, D. H., "The Effect of Surface Roughness on the Characteristics of the Aerofoils NACA 0012 and RAF 34," Aeronautical Research Council, ARC R&M 1708, Feb. 1936.

[19]Young, A. D., "The Drag Effects of Roughness at High Sub-Critical Speeds," *Journal of the Royal Aeronautical Society*, Aug. 1950, pp. 534–540.

[20]Bammert, K., and Sandstede, H., "Measurements Concerning the Influence of Surface Roughness and Profile Changes on the Performance of Gas Turbines," *Journal of Engineering for Power*, Vol. 94, No. 3, 1972, pp. 207–213.

[21]Bammert, K., and Milsch, R., "Boundary Layers on Rough Compressor Blades," American Society of Mechanical Engineers, ASME Paper 72-GT-48, March 1972.

[22]Bammert, K., and Sandstede, H., "Influences of Manufacturing Tolerances and Surface Roughness of Blades on the Performance of Turbines," *Journal of Engineering for Power*, Vol. 98, No. 1, 1976, pp. 29–36.

[23]Koch, C. C., and Smith, L. H., "Loss Sources and Magnitudes in Axial-Flow Compressors," *Journal of Engineering for Power*, Vol. 98, No. 3, 1976, pp. 411–424.

[24]Schaffler, A., "Experimental and Analytical Investigation of the Effects of Reynolds Number and Blade Surface Roughness on Multistage Axial Flow Compressors," *Journal of Engineering for Power*, Vol. 102, No. 1, 1980, pp. 5–13.

[25]Bammert, K., and Woelk, G. U., "The Influence of the Blading Surface Roughness on the Aerodynamic Behavior and Characteristic of an Axial Compressor," *Journal of Engineering for Power*, Vol. 102, No. 2, 1980, pp. 283–287.

[26]Hirsch, C., and Denton, J. D. (ed), "Survey on the Effects of Blade Surface Roughness on Compressor Performance," *Through Flow Calculations in Axial Turbomachines*, Advisory Rept. 175, AGARD, Oct. 1981, pp. 171–180.

[27]Tanis, F. J., "Roughness Effects on Compressor Blade Performance in Cascade at High Reynolds Number," Air Force Inst. of Technology, Rept. AFIT/GAE/AA/83D-23, Wright–Patterson AFB, OH, Nov. 1983.

[28]Moe, G. P., "Influence of Surface Roughness on Compressor Blades at High Reynolds Number in a Two-Dimensional Cascade," Air Force Inst. of Technology, Rept. AFIT/GAE/AA/84D-19, Wright–Patterson AFB, OH, Dec. 1984.

[29]Williams, L. D., "Effects of Surface Roughness on Pressure Distribution and Boundary Layer over Compressor Blades at High Reynolds Number in a Two-Dimensional Cascade," Air Force Inst. of Technology, Rept. AFIT/GAE/AA/85D-17, Wright–Patterson AFB, OH, Dec. 1985.

[30]Acharya, M., Bornstein, J., and Escudier, M. P., "Turbulent Boundary Layers on Rough Surfaces," *Experiments in Fluids*, Vol. 4, No. 1, 1986, pp. 33–47.

[31]Feiereisen, W. J., and Acharya, M., "Modeling of Transition and Surface Roughness Effects in Boundary-Layer Flows," *AIAA Journal*, Vol. 24, No. 10, 1986, pp. 1642–1649.

[32]Brumby, R. E., "The Effect of Wing Ice Contamination on Essential Flight Characteristics," Paper 2, CP-496, AGARD, Toulouse, France, April 1991.

[33]Boer, J. N., "Aerodynamic Degradation Due to Distributed Roughness on High Lift Configuration," AIAA Paper 93-0028, Jan. 1993.

[34]Valarezo, W. O., Lynch, F. T., and McGhee, R. J., "Aerodynamic Performance Effects due to Small Leading-Edge Ice (Roughness) on Wings and Tails," *Journal of Aircraft*, Vol. 30, No. 6, 1993, pp. 807–812.

[35]Morgan, H. L., Ferris, J. C., and McGhee, R. J., "A Study of High-Lift Airfoils at High Reynolds Numbers in the Langley Low-Turbulence Pressure Tunnel," NASA TM 89125, July 1987.

[36]Schairer, E. T., Mehta, R. D., Olsen, M. E., Hand, L. A., Bell, J. H., Whittaker, P. J., and Morgan, D. G., "The Effects of Thin Paint Coatings on the Aerodynamics of Semi-Span Wings," AIAA Paper 98-0587, Jan. 1998.

[37]Olsen, M. E., Driver, D. M., Schairer, E. T., and Naughton, J., "The ROCK (AST-1) Wing: Design, Experiment and Computation," AIAA Paper 2000-0670, Jan. 2000.

[38]McDevitt, J. B., Polek, T. E., and Hand, L. A., "A New Facility and Technique for Two-Dimensional Aerodynamic Testing," *Journal of Aircraft*, Vol. 20, No. 6, 1983, pp. 543–551.

[39]Puklin, E., Carlson, B., Gouin, S., Costin, C., and Green, E., "Ideality of Pressure-Sensitive Paint. I. Platinum Tetra(pentafluorophenl)porphine in Fluoroacrylic Polymer," *Journal of Applied Polymer Science*, Vol. 77, No. 13, 2000, pp. 2795–2804.

R. P. Lucht
Associate Editor